


Original Article

## Comparative Metagenomic Analysis of the Nasopharyngeal Microbiome in Healthy and Community-Acquired Pneumonia Pediatric Patients

Nada Ahmed<sup>1</sup>, Samah El-Sayed<sup>1</sup>, Samar Solyman<sup>1</sup>, Marwa Azab<sup>1</sup>, Salah Abdalla<sup>1</sup>, Shymaa Enany<sup>1</sup> , Amro Hanora<sup>1</sup>, Samira Zakeer<sup>1</sup>

Department of Microbiology & Immunology, Suez Canal University, Ismailia, Egypt.



**\*Corresponding author:**  
Prof. Amro Hanora,  
Department of Microbiology  
& Immunology, Suez Canal  
University, Ismailia, Egypt.

[a.hanora@pharm.suez.edu.eg](mailto:a.hanora@pharm.suez.edu.eg)

Received: 28 June 2025

Accepted: 30 July 2025

Published: 18 September 2025

DOI

[10.25259/STN\\_5\\_2025](https://doi.org/10.25259/STN_5_2025)

Quick Response Code:



Supplementary available  
on: [https://doi.org/10.25259/  
STN\\_5\\_2025](https://doi.org/10.25259/STN_5_2025)

### ABSTRACT

**Objective:** This study investigated the nasopharyngeal microbiome in Egyptian children with community-acquired pneumonia (CAP), comparing it with that of healthy children and their mothers, to better understand its role in disease progression and potential diagnostic value.

**Material and Methods:** Nasopharyngeal swabs from 31 participants were analyzed using shotgun metagenomic sequencing and bioinformatics to profile microbial communities and their functional potential.

**Results:** Children with CAP showed higher levels of pathogens such as *Moraxella catarrhalis* and *Streptococcus pneumoniae*, alongside a marked reduction in beneficial *Dolosigranulum pigrum*. Healthy children displayed a balanced community dominated by *Dolosigranulum pigrum* and *Corynebacterium* species, while mothers' microbiomes were enriched with *Cutibacterium acnes*. Functional profiling revealed CAP-associated enrichment of specific metabolic pathways, indicating possible therapeutic targets.

**Conclusion:** Alterations in the nasopharyngeal microbiota appear to be closely linked to pediatric CAP, highlighting its potential role in early diagnosis and informing future treatment approaches

**Keywords:** Biomarkers, Community-acquired pneumonia, Metagenomics, Nasopharyngeal microbiome

### 1. INTRODUCTION

The human microbiome, which encompasses commensal, symbiotic, and pathogenic microorganisms, plays a vital role in maintaining immune function and overall well-being<sup>[1]</sup>. The nasopharyngeal microbiota is particularly important in pediatric respiratory health.<sup>[2]</sup> The nasopharyngeal niche serves as both a reservoir for commensals and a gateway for pathogens, influencing susceptibility to respiratory infections through microbial interactions at the mucosal interface.<sup>[3]</sup> Dysbiosis in this niche has been linked to increased carriage of pathogens like *Streptococcus pneumoniae* and *Moraxella catarrhalis*, contributing to respiratory diseases such as sinusitis, asthma, and community-acquired pneumonia (CAP).<sup>[4]</sup>

The respiratory microbiome is a diverse community of bacteria, viruses, fungi, and eukaryotic organisms that inhabit the mucosal surfaces of the respiratory system. It interacts with the host and external factors, playing a crucial role in innate and adaptive immunity and protecting the host from invasive infections. Strong correlations exist between microbiome characteristics and disease

This is an open-access article distributed under the terms of the Creative Commons Attribution-Non Commercial-Share Alike 4.0 License, which allows others to remix, transform, and build upon the work non-commercially, as long as the author is credited and the new creations are licensed under the identical terms.

©2025 Published by Scientific Scholar on behalf of Science and Technology Nexus

risk.<sup>[5]</sup> Pneumonia is the leading global cause of death among children, with an 18% fatality rate. Pneumonia is the most common cause of death in children under five years of age. In the United States, over 100,000 pediatric hospitalizations occur annually, contributing to high antibiotic usage and costly hospital stays. There are 15.7 hospital-acquired cases of pneumonia for every 10,000 children, with higher rates among those younger than two.<sup>[6]</sup> Pneumonia causes roughly 19% of under-five mortality in Egypt, and 10% of child deaths in some locations. Community-acquired pneumonia (CAP) is a major reason for paediatric hospital admissions, with CAP prevalence reaching nearly 17-22% in Delta region studies.<sup>[7]</sup> Common causative agents include *Haemophilus influenzae*, *Streptococcus pneumoniae*, viruses, and atypical bacteria. Distinguishing between bacterial, viral, and atypical pneumonia can be challenging due to their often-overlapping clinical manifestations.<sup>[8]</sup>

Shotgun metagenomic sequencing eliminates the need for target-region amplification, as well as microbial isolation and culture, by analyzing all genomic DNA present in a sample. In natural environments, it is estimated that more than 99% of all microorganisms cannot be cultured using standard laboratory methods—these include the so-called “microbial dark matter” that can only be accessed through culture-independent approaches.<sup>[9]</sup> Unlike targeted amplicon sequencing (such as 16S rRNA, ITS, or 18S), which only captures specific marker genes, shotgun metagenomics provides comprehensive taxonomic resolution, functional insight across all microbial kingdoms in a sample, and the detection of novel pathogens, enhancing diagnostic yield in complex infections.<sup>[9]</sup>

The study examines the taxonomic diversity and metabolic features of the nasopharyngeal microbiome in children with community-acquired pneumonia (CAP), as well as in healthy children and their mothers, to identify the core microbiome and evaluate potential interactions, which may aid in the development of early diagnostic markers.

## 2. MATERIAL & METHODS

### 2.1. Study design

#### 2.1.1. Subject recruitment and specimen collection

The study was conducted in Egypt, in the city of 10th of Ramadan, at Ibn Sina Hospital and Al-Rashad Hospital. Nasopharyngeal swabs were collected from 31 subjects, including 11 children diagnosed with community-acquired pneumonia (CAP), aged from birth to 24 months, over six months from December 2022 to May 2023. Additionally, swabs were taken from 10 healthy children, serving as the control group. Simultaneous swabs were also obtained from

the mothers to evaluate maternal carriage to infant carriage, with 10 maternal samples collected. The samples were categorized into maternal, healthy children, and CAP groups. Demographic data and Clinical characteristics of the children with CAP are summarized in Supplementary Table 1. The inclusion of only healthy mothers minimized confounding variables such as illness, recent antibiotic use, or immune impairment. This design allowed assessment of microbiome transitions between healthy children and their mothers under stable health conditions. Participants were excluded if they had used antibiotics within six weeks, had a history of cancer, consumed high doses of commercial probiotics, or tested positive for HIV, HBV, or HCV. Individuals known to be positive for HIV, HBV, or HCV were excluded due to chronic immune impairment affecting microbiome composition. The study aimed to capture the nasopharyngeal microbiome at the early stage of clinical presentation before initiating antibiotic treatment.

### 2.2. DNA extraction

Nasopharyngeal swabs were vortexed, and sterile microcentrifuge tubes were used to extract genomic DNA using the DNeasy PowerSoil Pro DNA Isolation Kit (Qiagen, Valencia, CA, Cat. No. 47016-250). DNA quality and concentration were assessed using two complementary systems: Implen NanoPhotometer P330 (minimal sample volume: 0.3 µL; spectrum range: 190–1100 nm) and Thermo Fisher NanoDrop 2000 (≥0.5 µL; range: 190–840 nm). The study used two types of negative controls to ensure the integrity of low-biomass DNA samples: extraction blanks and no-template buffer controls. Extraction blanks were sterile swabs without biological material to detect background contamination from reagents or kits, while no-template buffer controls were empty tubes containing extraction buffer to uncover contamination introduced during handling or pipetting.

### 2.3. High-throughput sequencing

Shotgun metagenomic sequencing was conducted on 31 samples at IGA Technology Services using the MiSeq Reporter v2.3 workflow (Illumina) in Udine, Italy. DNA concentration was measured with a Qubit 2.0 Fluorometer (Invitrogen, Carlsbad, CA) to ensure a sufficient quantity (10–100 ng/µl) for processing. The quality of the libraries was assessed using the Agilent 2100 Bioanalyzer High Sensitivity DNA test (Agilent Technologies, Santa Clara, CA).

### 2.4. Metagenomic analysis

Reads were processed using Bcl2Fastq for format conversions and demultiplexing, followed by adapter removal with

Cutadapt<sup>[10]</sup> and quality filtering using FastQC<sup>[11]</sup> and Trimmomatic.<sup>[12]</sup> The study used Bowtie2<sup>[13]</sup> to minimize human DNA contamination in respiratory metagenomics studies. Preprocessed reads were aligned against the GRCh38 reference genome. The study successfully removed human DNA from non-host microbial sequences by filtering out reads aligning with the human genome, achieving 95–98.8% human retention, and cross-checking sample subsets for residual human content by remapping unmapped reads to the human genome. The assembly was conducted with SPAdes version 3.11.1.<sup>[14]</sup> A reference database of annotated protein sequences (NCBI-nr) was employed to align reads with the Diamond 0.9 aligner tool.<sup>[15]</sup> MEGAN software was utilized to analyze sequence data, generate taxonomy tables, and calculate alpha diversity metrics. Functional data analysis incorporated KEGG<sup>[16]</sup> and EC databases<sup>[17]</sup> with biomarker discovery supported by LEfSe.<sup>[18]</sup> Beta diversity patterns were examined using the Bray-Curtis index, with distance matrices calculated through cluster analysis in MEGAN.<sup>[19]</sup> The visualization of specific functional characteristics of the nasopharyngeal bacterial community, focusing on super pathways, was performed using the Microbiome Analyst online platform (<https://www.microbiomeanalyst.ca/>).<sup>[20]</sup>

## 2.5. Statistical analysis

Statistical analyses were conducted using R Package version 3.1.2.<sup>[21]</sup> Differential abundance was assessed using the one-way ANOVA across Healthy, CAP, and Mothers groups, followed by Tukey's HSD post hoc tests to identify specific group differences for each taxon. Diversity estimation was based on non-rarefied data, and ANOVA was employed to compare species across sample groups. The significance of beta diversity was evaluated using the Bray-Curtis index in conjunction with the PERMANOVA test. The Spearman correlation coefficient was utilized to analyze correlations within the microbiota. Biomarker discovery was performed using the Linear Discriminant Analysis Effect Size (LEfSe)<sup>[22]</sup> approach, with an effect size cutoff established at a logarithmic LDA score greater than 2.

## 3. RESULTS AND DISCUSSION

The whole genome shotgun sequencing generated an average of 10 million raw reads per sample, with 98% meeting quality standards (Phred scores  $\geq 30$ ). Non-human reads, which comprised 1.2% to 5% of the total, were analyzed. After adapter removal and quality filtering, high-quality reads were assembled for downstream analysis: 175,839 reads for maternal/healthy groups and 204,178 reads for CAP/healthy child groups.

### 3.1. Taxonomic composition analysis

#### 3.1.1. Microbial composition at the genus level

In the maternal group, the predominant genera in the nasopharyngeal communities were *Corynebacterium* (61%), *Dolosigranulum* (16%), *Moraxella* (2%), *Cutibacterium* (2%), *Staphylococcus* (1%), and *Streptococcus* (1%). In contrast, the healthy child group was primarily characterized by *Dolosigranulum* (66%), followed by *Corynebacterium* and *Moraxella* (10% each). A total of ten genera were identified as predominant across the groups studied, as shown in the Supplementary Figure 1. In this study, *Veillonella* was present at a low abundance in the healthy group (0.27%). The community-acquired pneumonia (CAP) group exhibited a significant increase in the prevalence of *Moraxella* (40%) and *Streptococcus* (26%) ( $P$ -value = 0.0022434, FDR = 0.0078519, and  $P$ -value = 0.0054579, FDR = 0.012735). Both *Dolosigranulum* and *Corynebacterium* showed significantly reduced abundances in the CAP group (13% and 8%, respectively;  $P$ -value = 0.0020583 and FDR = 0.020583). Additionally, a significant difference in *Dolosigranulum* abundance was observed between the healthy child and maternal groups ( $P$ -value = 0.005196 and FDR = 0.041568).

#### 3.1.2. The relative composition of nasal microbiota at the species level

The species composition in the CAP group differed significantly from that of the healthy child group. The CAP group was predominantly composed of *Moraxella catarrhalis* (34%), *Streptococcus pneumoniae* (9%), *Haemophilus influenzae* (6%), *Moraxella nonliquefaciens* (6%), and *Cupriavidus pauculus* (1%). In contrast, the healthy child group exhibited a higher prevalence of *Dolosigranulum pigrum* (93%), *Corynebacterium pseudodiphtheriticum* (2%), and *Corynebacterium propinquum* (1%). Similarly, in the maternal group, *Dolosigranulum pigrum* was also abundant (40%), along with *Corynebacterium propinquum* (32%), *Moraxella nonliquefaciens* (7%), and *Corynebacterium macginleyi* (3%), as illustrated in Figure 1.

*Moraxella catarrhalis* was the only species with a significant difference across groups: ANOVA  $F = 8.55$ ,  $p = 0.00126$ . Tukey's HSD revealed significantly higher abundance in CAP compared to Healthy. No significant differences were observed between Mothers vs. CAP or Mothers vs. Healthy. Statistics are summarized in Supplementary Table 2 and supplementary figure 2.

### 3.2. Diversity analysis

#### 3.2.1. Alpha diversity analysis

We quantified microbial diversity using three established indices: Observed-species, Shannon index, and Simpson

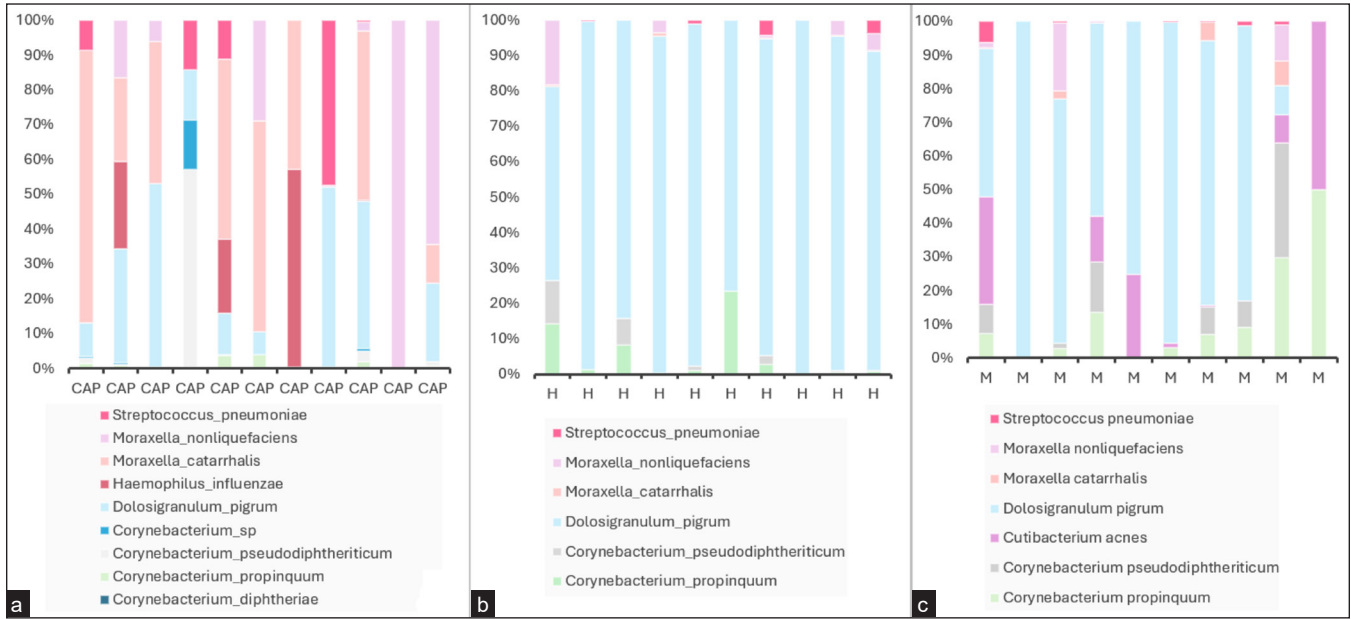


**Figure 1:** Relative abundance of the most predominant species, represented by bar charts across different groups (M: Maternal group; H: Healthy child group; CAP: Community-acquired pneumonia group). (a) Relative abundance in the CAP group, (b) Relative abundance in the healthy child group, (c) Relative abundance in the maternal group.

index. A total of 173 species were identified in the healthy and diseased child groups, while 234 species were found in the maternal and healthy child groups. Rarefactions to a depth of 120,000 reads have been carried out. The rarefaction curve indicates that the sampling depth was sufficient. Across all metrics, the mothers (M) group had the highest alpha diversity, healthy children (H) were intermediate, and CAP patients displayed the lowest diversity [Supplementary Figure 4].

**3.2.2. Beta diversity analysis**

Divergences between the maternal group and the healthy child groups were found to be statistically significant, as determined by the PERMANOVA test ( $p$ -value = 0.001). Additionally, statistically significant clustering was observed between the healthy child and CAP groups using the same test ( $p$ -value = 0.014). The Principal Coordinates Analysis (PCoA) of Bray-Curtis dissimilarities among the studied groups is presented in Figure 2.

**3.2.3. Core nasopharyngeal microbiome**

The core microbiome, defined as the species present in at least 80% of all samples, comprised 170 species. Notable species within this core group included *Corynebacterium propinquum*, *Dolosigranulum pigrum*, *Corynebacterium pseudodiphtheriticum*, *Moraxella nonliquefaciens*, *Moraxella catarrhalis*, *Bacillus thuringiensis*, and *Moraxella lacunata*. Four species were common across all groups: *Corynebacterium propinquum*,

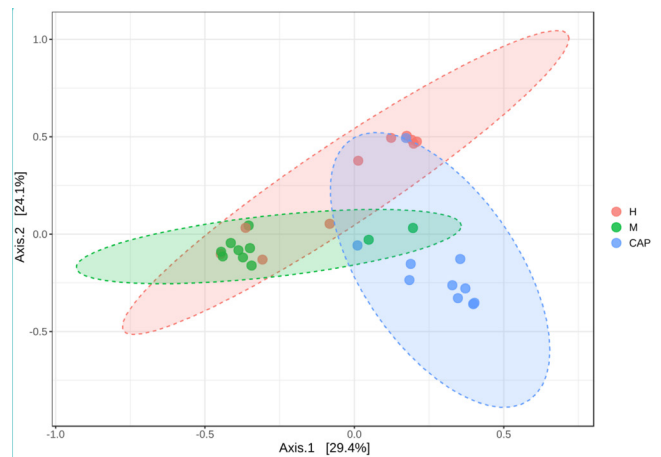


**Figure 2:** Principal coordinates analysis (PCoA) of the Bray-Curtis distance matrix of nasopharyngeal microbial community structures across groups. Statistical analysis revealed significant differences among the groups studied, with distinct clustering observed (M: Maternal group; H: Healthy child group; CAP: Community-acquired pneumonia group).

*Moraxella nonliquefaciens*, *Nocardioides agariphilus*, and *Escherichia coli*. The CAP group exhibited 24 distinctive species, while the healthy child group had two, and the maternal group had 39 unique species [Supplementary Figure 3].

**3.2.4. Microbial interactions**

Correlation analyses using the Spearman correlation coefficient were conducted across all samples to examine

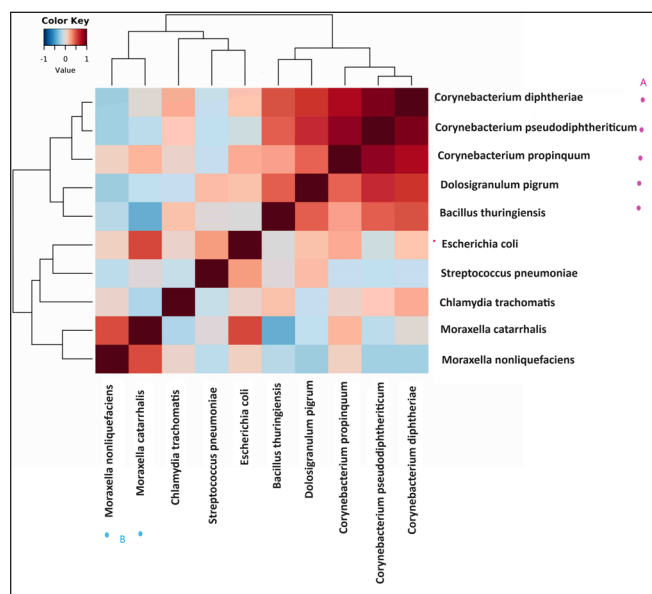


**Figure 3:** Correlation plot illustrates the pairwise correlations of the most predominant genera of the nasal microbiota. Correlations were assessed using the Spearman rank correlation coefficient (two-tailed). Two major clusters have been identified: members of Cluster A are represented by magenta dots, while blue dots indicate members of Cluster B. Dark red indicates strong positive correlations, and dark blue represents negative correlations. Significant correlations were determined at  $p < 0.05$  after Benjamini–Hochberg false discovery rate (FDR) correction for multiple comparisons. The strongest positive correlation was observed between *Moraxella catarrhalis* and *Moraxella nonliquefaciens* ( $r = 0.45$ ,  $p = 0.003$ , FDR-adjusted  $p = 0.012$ ), while a significant negative correlation was identified between *Dolosigranulum pigrum* and *Moraxella catarrhalis* ( $r = -0.41$ ,  $p = 0.004$ , FDR-adjusted  $p = 0.015$ ).

interactions among bacterial populations from the phyla Actinomycetota, Proteobacteria, and Firmicutes. Significant positive correlations ( $r = 0.89$ ) were observed among bacteria from the genera *Corynebacterium*, *Bacillus*, *Streptococcus*, *Corynebacterium*, and *Moraxella*, with members of the Actinomycetota and Firmicutes exhibiting a significant positive correlation ( $r = 0.89$ ). Two major clusters were identified, representing members of the major phyla that were positively correlated [Figure 3]. Cluster A: *Corynebacterium pseudodiphtheriticum*, *Corynebacterium propinquum*, (belonging to phylum Actinomycetota), *Corynebacterium diphtheriae*, *Dolosigranulum pigrum*, and *Bacillus thuringiensis* existed with a significantly positive correlation to each other and inversely correlated to species of clusters B, except *Corynebacterium propinquum* and *Corynebacterium diphtheriae* (in the phylum Actinomycetota). Cluster B: *Moraxella catarrhalis* and *Moraxella nonliquefaciens* (in the phylum Pseudomonadota) are significantly positively correlated to each other and negatively correlated to genera of cluster A, except *Corynebacterium propinquum* and *Corynebacterium diphtheriae*. The strongest positive

correlation at the species level was observed between *Moraxella catarrhalis* and *Moraxella nonliquefaciens* ( $r = 0.45$ ) within Cluster B. In contrast, a significant negative correlation was identified between *Dolosigranulum pigrum* and *Moraxella catarrhalis*, suggesting competition between these species. Furthermore, *Dolosigranulum pigrum* also exhibited a negative correlation with *Moraxella nonliquefaciens*.

### 3.2.5. Functional annotation of protein database

The assessment of enzyme classes revealed differences in the relative abundance of predicted enzyme functions between the groups. The healthy child group exhibited higher levels of Hydrolase (29%), Ligase (17%), and Oxidoreductase (11%) compared to the CAP group, which showed lower levels of these enzymes (24%, 6%, and 9%, respectively). In contrast, the CAP group demonstrated a greater abundance of Translocase (11%) and Lyases (4%) compared to the healthy child group, which had lower levels of these enzymes (7% and 2%, respectively).

Univariate analysis indicated a significant increase in Lyases in the CAP group ( $P$ -value: 0.004295; FDR: 0.03006). The healthy child group exhibited higher levels of oxidoreductase, particularly L-lactate dehydrogenase (EC 1.1.1.27), compared to the CAP group. The maternal group demonstrated an increased abundance of Transferase, with an average abundance of 30%, as shown in Supplementary Table 3.

### 3.2.6. Functional prediction using KEGG gene function pathways

An analysis of predicted functional profiles using the KEGG database identified 20 distinct gene function pathways between the CAP and healthy child groups. These pathways included six metabolic pathways, one pathway related to genetic information processing, two pathways associated with environmental information processing, and others linked to cellular processes. The CAP group exhibited a higher abundance of pathways associated with human diseases (3% compared to 1%). In comparison, the healthy child group demonstrated more pathways related to environmental information processing (5% versus 3%). Pathway enrichment analysis revealed distinct metabolic profiles across groups [Supplementary Figure 5]. In the CAP group, enriched pathways were primarily associated with carbohydrate, amino acid, and lipid metabolism, as well as membrane transport. In contrast, the healthy child group showed greater enrichment in genetic information processing pathways, including replication, repair, and translation. Metabolic functions in this group were also linked to energy metabolism, cofactors, vitamins, nucleotides, carbohydrates, amino acids, lipids, enzyme families, and glycan biosynthesis. The maternal

group exhibited a higher representation of pathways related to signaling and cellular processes, as well as carbohydrate metabolism (15% and 14%, respectively). Significant metabolic pathways between the CAP and the healthy child groups are summarized in the Supplementary Table 4. However, no significant differences in pathway enrichment were observed between the maternal and child groups

Supplementary Figure 5 illustrates the heat map plot of enriched functional features of the nasopharyngeal bacterial community, focusing on the super pathways in the studied groups (community-acquired pneumonia [CAP] vs healthy controls). Although no statistically significant differences were observed at the superpathway level, several individual pathways demonstrated significant differences between groups. Statistical differences were assessed using the Kruskal–Wallis test ( $p < 0.05$ ), and  $p$ -values were adjusted for multiple testing using the Benjamini–Hochberg false discovery rate (FDR) method.

### 3.2.7. Identification of biomarkers and discriminative taxa

LEfSe analysis identified *D. pigrum* (healthy group;  $P = 0.0001$ ; LDA = 6.51) and *M. catarrhalis* (CAP group;  $P = 0.018$ ; LDA = 6.21) as the only significant biomarkers, as illustrated in Supplementary Figure 6a. To identify pathways with significant variations in abundance among the groups, KEGG gene annotation was utilized, and LEfSe analysis was conducted. Persistent differences in KEGG pathway patterns between the various groups were observed [Supplementary Figure 6b].

Significant pathways related to signaling and cellular processes, including transporters such as the translocation and assembly module TamB (K09800), iron complex outer membrane receptor protein (K02014), hemoglobin transferrin lactoferrin receptor protein (K16087), lactate permease (K03303), and LPS assembly protein (K04744), were found to be significant in the CAP group [Supplementary Table 4].

### 3.3. Discussion

The study analyzed differences in nasopharyngeal microbiome structure between pediatric patients with community-acquired pneumonia and healthy children, as well as between healthy children and their mothers, focusing on potential microbial transmission and the influence of maternal microbiota. Previous research suggests that the microbiomes of healthy children and their mothers often share similarities due to vertical microbial transmission and shared environmental exposures, establishing a stable core microbiome early in life that persists despite age differences.<sup>[23]</sup>

Consistent with prior studies, our data show that healthy children harbor a balanced microbiome, dominated

by beneficial taxa such as *Dolosigranulum pigrum* and *Corynebacterium* species.<sup>[24]</sup> *Dolosigranulum pigrum*, a lactic acid bacterium known for inhibiting pathogenic microorganisms and supporting immune function,<sup>[25]</sup> was abundant in healthy children, suggesting its role in maintaining nasopharyngeal homeostasis when combined with *Corynebacterium* spp. The presence of *Veillonella*, another lactate-rich genus, may further enhance this protective microbial community. These findings reinforce the notion that certain taxa could serve as targets for preventive and therapeutic strategies.<sup>[26]</sup>

In contrast, children with CAP exhibited reduced microbial diversity and an enrichment of potential respiratory pathogens, consistent with the concept of microbiome disruption and decreased colonization resistance.<sup>[27]</sup> This dysbiotic shift has been reported in other respiratory infections and may have diagnostic value in distinguishing children at risk of CAP.<sup>[28]</sup> Our data suggest that microbial alterations could potentially serve as biomarkers for early identification and intervention, which could help reduce unnecessary antibiotic use; however, further validation in larger cohorts is needed to establish clinical utility.

Within the CAP group, two distinct *Moraxella*-dominated microbiota profiles were identified: one dominated by *Moraxella catarrhalis* and another by *Moraxella nonliquefaciens*.<sup>[29]</sup> *Moraxella catarrhalis* is a well-known respiratory pathogen associated with chronic obstructive pulmonary disease, pneumonia, and otitis media.<sup>[30]</sup> Although *Moraxella nonliquefaciens* is less frequently reported, it has been implicated in opportunistic infections and is often underrecognized due to misidentification and its inherent antibiotic resistance.<sup>[31]</sup>

Notably, we observed the increased relative abundance of *Moraxella* spp. compared with *Streptococcus pneumoniae* in the CAP group, *Moraxella* species are relative to *Streptococcus pneumoniae*, particularly *M. catarrhalis* and *Haemophilus influenzae*. External factors such as pneumococcal vaccination programs may have contributed to this epidemiological shift by altering *S. pneumoniae* serotype distribution, creating ecological niches for other pathogens.<sup>[31]</sup> Future studies should specifically investigate how vaccination practices influence nasopharyngeal community composition.

Correlative network analysis revealed a positive association between *Corynebacterium pseudodiphtheriticum* and *Dolosigranulum pigrum* in healthy children, reflecting their cooperative role in maintaining nasopharyngeal ecosystem stability. Conversely, a significant negative correlation was observed between *Dolosigranulum pigrum* and *Moraxella catarrhalis*, suggesting competitive interactions. Functional prediction analysis further showed that healthy children harbored a higher prevalence of oxidoreductase subclasses,

particularly lactate-producing enzymes, which are known to lower pH and enhance antimicrobial defense mechanisms. These findings suggest that metabolic outputs of commensal taxa may contribute to colonization resistance and could represent novel therapeutic targets.

Our study also highlights the potential role of iron acquisition pathways in CAP pathogenesis.<sup>[32]</sup> Gram-negative respiratory pathogens such as *M. catarrhalis* exploit host-derived iron-binding proteins (e.g., transferrin and lactoferrin) for growth and colonization. We observed increased abundance of transferrin and lactoferrin receptor pathways in the CAP group, suggesting that enhanced iron-scavenging capabilities may support pathogen persistence and virulence. These host-microbe interactions represent promising avenues for the development of vaccines and therapeutics targeting microbial nutrient acquisition strategies.

#### 4. CONCLUSION

This study demonstrates that the nasopharyngeal microbiota of healthy children is dominated by *Dolosigranulum pigrum* and *Corynebacterium* spp., taxa that appear to work synergistically to maintain mucosal stability and resist pathogen colonization. In contrast, children with CAP showed reduced diversity and increased abundance of *Moraxella catarrhalis*, *M. nonliquefaciens*, and *S. pneumoniae*. Negative correlations between *Dolosigranulum pigrum* and *Moraxella* species suggest competitive interactions influencing disease risk.

#### Future directions

Longitudinal studies with larger and more diverse cohorts are needed to elucidate the temporal relationship between microbiome disruption and CAP onset. Incorporating additional layers of data, such as metabolomics and host immune responses, will help clarify the biological mechanisms underlying these shifts. Experimental studies are also needed to test whether protective species like *Dolosigranulum pigrum* could be used as probiotics or therapeutic interventions. Understanding how factors like vaccination and antibiotic use shape the nasopharyngeal microbiome could further guide strategies to prevent CAP in children.

#### Limitations of the study

The primary limitation of this study is the modest sample size, which, while consistent with other exploratory microbiome research, limits statistical power and generalizability. All findings should be validated in larger cohorts. Despite these constraints, the study provides valuable preliminary evidence linking nasopharyngeal microbiome composition and function to CAP in children, offering a foundation for future research.

**Ethical Approval:** The study was approved by the Scientific Research Ethics Committee at the Faculty of Pharmacy, Suez Canal University, Egypt (Reference Number: 202012PHD4), 14 December 2020. All experiments were conducted according to relevant guidelines. This study was conducted in accordance with the principles of the Declaration of Helsinki.

**Declaration of patient consent:** The authors certify that they have obtained all appropriate patient consent.

**Financial support and sponsorship:** Academy of Scientific Research and Technology, Project No. 85D/2021

**Conflicts of interest:** There are no conflicts of interest.

**Use of artificial intelligence (AI)-assisted technology for manuscript preparation:** The authors confirm that there was no use of artificial intelligence (AI)-assisted technology for assisting in the writing or editing of the manuscript, and no images were manipulated using AI.

#### REFERENCES

- Pérez-Cobas, A.E., *et al.*, 2023. Cell Reports Medicine, **4**, 101167.
- Pol, S., *et al.*, 2024. mBio, **15**, e0078424
- Dimitri-Pinheiro S, *et al.*, 2020. Allergy Rhinol (Providence). **11**:2152656720911605.
- Drigot, Z.G., *et al.*, 2024. Current Opinion in Microbiology, **77**, 102428.
- de Steenhuijsen Pijters, W.A.A., *et al.*, 2015. Philosophical Transactions of the Royal Society of London. Series B, Biological Sciences, **370**, 20140294.
- Popovsky, E.Y., *et al.*, 2022. Encyclopedia of Respiratory Medicine, **6**, 119-131.
- Fadl, N., *et al.*, 2020. Eastern Mediterranean Health Journal, **26**, 1042-1051.
- Zedan, M., *et al.*, 2025. The Egyptian Journal of Bronchology, **19**, 2.
- Quince, C., *et al.*, 2017. Nature Biotechnology, **35**, 833-844.
- Martin, M., *et al.*, 2011. EMBnet Journal, **17**, 10.
- Babraham Bioinformatics. FastQC: A quality control tool for high throughput sequence data. Cambridge (UK): Babraham Institute; Available from: <https://www.bioinformatics.babraham.ac.uk/projects/fastqc/> [Last accessed: 15 February 2025].
- Bolger, A.M., *et al.*, 2014. Bioinformatics, **30**, 2114-2120.
- Langmead, B., *et al.*, 2019. Bioinformatics, **35**, 421-432.
- Bankevich, A., *et al.*, 2012. Journal of Computational Biology, **19**, 455-477.
- Buchfink, B., *et al.*, 2015. Nature Methods, **12**, 59-60.
- Kanehisa, M., *et al.*, 2000. Nucleic Acids Research, **28**, 27-30.
- Webb, E.C., *et al.*, 1992. Recommendations of the Nomenclature Committee of the IUBMB on Enzyme Classification Available from: <https://iubmb.qmul.ac.uk/enzyme/> [Last accessed: 19 February 2025].
- Segata, N., *et al.*, 2011. Genome Biology, **12**, 1-18.
- Huson, D.H., *et al.*, 2007. Genome Research, **17**, 377-386.
- Chong, J., *et al.*, 2020. Nature Protocols, **15**, 799-821.
- Wickham, H., *et al.*, 2023. R Packages. O'Reilly Media, Inc., 382.
- Tharwat, A., *et al.*, 2017. AI Communications, **30**, 169-190.

23. Bogaert, D., *et al.*, 2023. *Cell Host Microbe*, **31**, 447-460.e6.
24. Mokoena, M.P., *et al.*, 2017. *Molecules*, **22**, 1255.
25. Brugger, S.D., *et al.*, 2020. *mSphere*, **5**, e00852-20.
26. Sherret, J., *et al.*, 2020. *Cureus*, **12**, e9770.
27. Man, W.H., *et al.*, 2019. *Lancet Respiratory Medicine*, **7**, 417-426.
28. Man, W.H., *et al.*, 2017. *Nature Reviews Microbiology*, **15**, 259-270.
29. Van den Munckhof, E.H.A., *et al.*, 2020. *Scientific Reports*, **10**, 8752.
30. Teo, S.M., *et al.*, 2015. *Cell Host Microbe*, **17**, 704-715
31. Bosch, A.A.T.M., *et al.*, 2016. *EBioMedicine*, **9**, 336-345
32. Chan, C., *et al.*, 2018. *Biometals*, **31**, 381-398.

**How to cite this article:** Ahmed N, El-Sayed S, Solyman S, Azab M, Abdalla S, Enany S, Hanora A, *et al.* Comparative Metagenomic Analysis of the Nasopharyngeal Microbiome in Healthy and Community-Acquired Pneumonia Pediatric Patients. *Sci Technol Nex.* 2025;1:16-23. doi: 10.25259/STN\_5\_2025